Progress In Electromagnetics Research M, Vol. 8, 153–162, 2009

A UTD ENHANCED PO-TDIE HYBRID ALGORITHM

Y. J. Qin, D. M. Zhou, J. G. He, and P. G. Liu

School of Electronic Science and Engineering
National University of Defense Technology
Changsha 410073, China

Abstract—A uniform geometrical theory of diffraction (UTD) enhanced physical optics and time domain integral equation (PO-TDIE) hybrid algorithm is proposed. UTD is applied to calculate the edge effect and to compensate the calculation error made by the PO current approximation. This method can improve the accuracy while maintaining the computational complexity, compared to PO-TDIE. Numerical result illustrates the validity and efficiency of the proposed method.

1. INTRODUCTION

In 1960s, marching-on in time solver (MOT) of Time Domain Integral Equation algorithm (TDIE) appeared for computing the transient response of conducting bodies [1]. However, it has suffered from very high computational cost. For a problem with N_s spatial and N_t temporal unknowns, the computational cost of the MOT solver is $O(N_t N_s^2)$. That means, in electrically large applications, the method is always impractical.

For this reason, people have developed various methods to accelerate TDIE algorithm: Dr. Walker have proposed a method to reduce the computational complexity via physical approximation [2, 3]; plane wave time domain (PWTD) algorithm [4] reduces the complexity of TDIE solution to $O(N_t N_s \log^2(N_s))$ [5]; time domain adaptive integral method (TD-AIM) is a fast solution techniques based on fast Fourier transform, which is developed by Yilmaz et al. [6, 7].

Another kind of fast solution techniques is hybrid method. To the best of our knowledge, PO-TDIE method [8, 9] is the only hybrid method in which people are interested currently. In this respect, hybrid methods have a great potential for development.

Corresponding author: Y. J. Qin (glsqyj@nudt.edu.cn).

According to the PO current approximation, the computational cost of full TDIE solver can be significantly decreased. However, this hybrid method has limitations: The accuracy is dependent on the complexity of the target's shape. If PO region contains sharp edges and corners, the calculation error will increase. The only way to increase the accuracy cannot be otherwise than putting the edges and corners into TDIE region. However, the computational cost will increase simultaneously.

In uniform geometrical theory of diffraction (UTD) [10], edges and corners are typical diffraction characteristics; therefore, if edges and corners in PO region could be solved by UTD, the calculation error of PO-TDIE will be reduced without increasing the computational cost. Sequentially, the computing capacity of the PO-TDIE hybrid method will be enhanced and the application range would be extended.

A novel UTD (in time domain version) enhanced PO-TDIE hybrid method (UTD-PO-TDIE) is proposed in this paper, which leads to accuracy enhancement while maintaining the computational complexity compared to PO-TDIE. A numerical example illustrates the efficiency and the accuracy of the proposed method.

2. PO-TDIE HYBRID METHOD

As the first step, the surface is divided into two parts: PO region and TDIE region. Since PO is only applicable to surface target, smooth surface parts are divided into PO region; the rest are divided into TDIE region, as shown in Figure 1. The popular RWG basis function [11] over triangular patches is employed as spatial basis function in surface part; the triangle basis function [12] is employed in wire part; the traditional surface-wire basis function [13] is employed in surface-wire junction.

The current density vectors can be expanded in PO and TDIE region, respectively:

$$\begin{cases} \mathbf{J}^{\mathrm{IE}}(\mathbf{r},t) \approx \sum\limits_{i=0}^{N_t} \sum\limits_{n}^{N_s^{\mathrm{IE}}} I_{n,i}^{\mathrm{IE}} \mathbf{f}_n^{\mathrm{IE}}(\mathbf{r})\, T_i(t) \\ \mathbf{J}^{\mathrm{PO}}(\mathbf{r},t) \approx \sum\limits_{i=0}^{N_t} \sum\limits_{n}^{N_s^{\mathrm{PO}}} I_{n,i}^{\mathrm{PO}} \mathbf{f}_n^{\mathrm{PO}}(\mathbf{r})\, T_i(t) \end{cases} \tag{1}$$

where, $\mathbf{f}_n^{\mathrm{IE}}(\mathbf{r})$ and $\mathbf{f}_n^{\mathrm{PO}}(\mathbf{r})$ denotes the spatial basis function in each region; $T(t)$ denotes the temporal basis function, and $T_i(t) = T(t - i\Delta t)\ t \geq 0$; $I_{n,i}$ means the current coefficient; N_s^{IE}, N_s^{PO} and

N_t are the spatial and temporal free degrees in the two regions, respectively.

Based on the boundary conditions for PEC, time domain electric field integral equation (TDEFIE) can be set up in TDIE region

$$\hat{\mathbf{n}} \times \hat{\mathbf{n}} \times \left[\mathbf{E}^s\left(\mathbf{J}^{\mathrm{IE}}(\mathbf{r},t)\right) + \mathbf{E}^s\left(\mathbf{J}^{\mathrm{PO}}(\mathbf{r},t)\right) + \mathbf{E}^i(\mathbf{r},t)\right] = 0 \tag{2}$$

where, $\hat{\mathbf{n}}$ denotes the outward normal vector of the surface; $\hat{\mathbf{n}} \times \hat{\mathbf{n}} \times [\,]$ indicates taking the tangential components of a vector; $\mathbf{E}^i(\mathbf{r},t)$ denotes the excitation.

And from the knowledge of PO, in PO region we have

$$\mathbf{J}^{\mathrm{PO}}(\mathbf{r},t) = \begin{cases} 2\hat{\mathbf{n}} \times \left[\mathbf{H}^s\left(\mathbf{J}^{\mathrm{IE}}(\mathbf{r},t)\right) + \mathbf{H}^i(\mathbf{r},t)\right] & \text{illuminated} \\ 0 & \text{shadowed} \end{cases} \tag{3}$$

Extending (2) (3), we obtain

$$\begin{aligned} &\hat{\mathbf{n}} \times \hat{\mathbf{n}} \times \mathbf{E}^i(\mathbf{r},t) \\ &= \hat{\mathbf{n}} \times \hat{\mathbf{n}} \times \left[\frac{\mu_0}{4\pi}\int_s \frac{1}{R}\frac{\partial \mathbf{J}^{\mathrm{IE}}(\mathbf{r}',\tau)}{\partial t}ds' - \frac{1}{4\pi\varepsilon_0}\nabla\int_s ds'\int_{-\infty}^{\tau}\frac{\nabla'\cdot\mathbf{J}^{\mathrm{IE}}(\mathbf{r}',t')}{R}dt'\right] \\ &\quad + \hat{\mathbf{n}} \times \hat{\mathbf{n}} \times \left[\frac{\mu_0}{4\pi}\int_s \frac{1}{R}\frac{\partial \mathbf{J}^{\mathrm{PO}}(\mathbf{r}',\tau)}{\partial t}ds' - \frac{1}{4\pi\varepsilon_0}\nabla\int_s ds'\int_{-\infty}^{\tau}\frac{\nabla'\cdot\mathbf{J}^{\mathrm{PO}}(\mathbf{r}',t')}{R}dt'\right] \end{aligned} \tag{4}$$

$$\begin{aligned} \hat{\mathbf{n}} \times \mathbf{H}^i(\mathbf{r},t) \;=\; & \frac{\mathbf{J}^{\mathrm{PO}}(\mathbf{r},t)}{2} - \hat{\mathbf{n}} \\ & \times \frac{1}{4\pi}\int_s \nabla \times \frac{\mathbf{J}^{\mathrm{IE}}(\mathbf{r}',\tau)}{R}ds' \text{ illuminated region} \end{aligned} \tag{5}$$

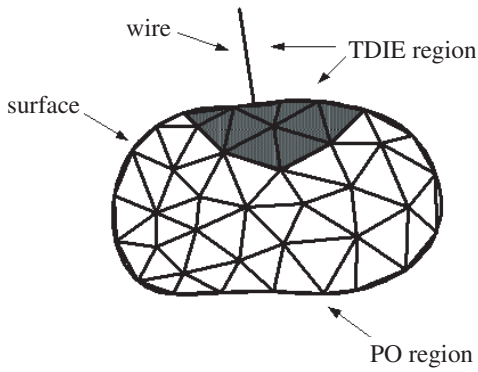

Figure 1. Partitioning of the analyzed model according to the PO-TDIE paradigm.

Applying spatial Galerkin testing and temporal δ testing, the following equation is obtained finally [8]:

$$\begin{bmatrix} \mathbf{Z}_0^{\text{IE-IE}} & \mathbf{Z}_0^{\text{IE-PO}} \\ \mathbf{Z}_0^{\text{PO-IE}} & \mathbf{C}_0^{\text{PO-PO}} \end{bmatrix} \cdot \begin{bmatrix} \mathbf{I}_j^{\text{IE}} \\ \mathbf{I}_j^{\text{PO}} \end{bmatrix} = \begin{bmatrix} \mathbf{V}_j^{\text{IE}} \\ \mathbf{V}_j^{\text{PO}} \end{bmatrix} - \sum_{i=1}^{j} \begin{bmatrix} \mathbf{Z}_i^{\text{IE-IE}} & \mathbf{Z}_i^{\text{IE-PO}} \\ \mathbf{Z}_i^{\text{PO-IE}} & \mathbf{C}_i^{\text{PO-PO}} \end{bmatrix} \cdot \begin{bmatrix} \mathbf{I}_{j-i}^{\text{IE}} \\ \mathbf{I}_{j-i}^{\text{PO}} \end{bmatrix} \tag{6}$$

where,

$$\mathbf{Z}_{i,mm}^{\text{IE-IE}} = \left\langle \mathbf{f}_m^{\text{IE}}(\mathbf{r}),\, \hat{\mathbf{n}} \times \hat{\mathbf{n}} \times \left[\frac{\mu_0}{4\pi} \int_s \frac{\mathbf{f}_n^{\text{IE}}(\mathbf{r}')}{R} \frac{\partial T\left(i\Delta t - R/c\right)}{\partial t} ds' - \frac{1}{4\pi\varepsilon_0} \nabla \int_s ds' \int_{-\infty}^{\tau} \frac{\nabla' \cdot \mathbf{f}_{\mathbf{n}}^{\text{IE}}(\mathbf{r}')}{R} T\left(i\Delta t - R/c\right) dt' \right] \right\rangle \tag{7}$$

means the mutual-interaction in TDIE region;

$$\mathbf{Z}_{i,mm}^{\text{IE-PO}} = \left\langle \mathbf{f}_m^{\text{IE}}(\mathbf{r}),\, \hat{\mathbf{n}} \times \hat{\mathbf{n}} \times \left[\frac{\mu_0}{4\pi} \int_s \frac{\mathbf{f}_n^{\text{PO}}(\mathbf{r}')}{R} \frac{\partial T\left(i\Delta t - R/c\right)}{\partial t} ds' - \frac{1}{4\pi\varepsilon_0} \nabla \int_s ds' \int_{-\infty}^{\tau} \frac{\nabla' \cdot \mathbf{f}_{\mathbf{n}}^{\text{PO}}(\mathbf{r}')}{R} T\left(i\Delta t - R/c\right) dt' \right] \right\rangle \tag{8}$$

means PO region's contribution to TDIE region;

$$\mathbf{Z}_{i,mm}^{\text{PO-IE}} = \left\langle \mathbf{f}_m^{\text{PO}}(\mathbf{r}), -\hat{\mathbf{n}} \times \nabla \times \frac{1}{4\pi} \int_s \frac{\mathbf{f}_n^{\text{IE}}(\mathbf{r}')}{R} T\left(i\Delta t - R/c\right) ds' \right\rangle \tag{9}$$

means TDIE region's contribution to PO region;

$$\mathbf{C}_{i,mm}^{\text{PO-PO}} = \frac{1}{2} \left\langle \mathbf{f}_m^{\text{PO}}(\mathbf{r}),\, \mathbf{f}_n^{\text{PO}}\left(\mathbf{r}'\right) T(i\Delta t) \right\rangle \tag{10}$$

means the expression of PO current approximation; and

$$\mathbf{V}_{j,m}^{\text{IE}} = \left\langle \mathbf{f}_m^{\text{IE}}(\mathbf{r}),\, \hat{\mathbf{n}} \times \hat{\mathbf{n}} \times \mathbf{E}^i(\mathbf{r}, t) \right\rangle \big|_{t=t_j} \tag{11}$$

$$\mathbf{V}_{j,m}^{\text{PO}} = \left\langle \mathbf{f}_m^{\text{PO}}(\mathbf{r}),\, \hat{\mathbf{n}} \times \mathbf{H}^i(\mathbf{r}, t) \right\rangle \big|_{t=t_j} \tag{12}$$

means the excitation in TDIE region and PO region, respectively.

Equation (6) is the formulation of PO-TDIE hybrid method. The reduction of computational cost, compared to the classical MOT solver, is achieved by neglecting the mutual interactions in PO region. Generally, the unknowns in PO region are of large proportion; therefore, the computational complexity of the impedance matrix will be reduced dramatically.

3. UTD ENHANCEMENT

In the theory of time domain version of UTD [14, 15] (TD-UTD), the total field is, at the observation point P_r

$$\mathbf{E}(\mathbf{r},t) = \mathbf{E}^i(\mathbf{r},t) + \mathbf{E}^d(\mathbf{r},t) \tag{13}$$

where, $\mathbf{E}^i(\mathbf{r},t)$ denotes the incident field; $\mathbf{E}^d(\mathbf{r},t)$ denotes the wedge diffracted field.

The expression of $\mathbf{E}^d(\mathbf{r},t)$ is as follows:

$$\mathbf{E}^d(r,t) = A(r)\int_{t_0}^{t-\frac{r}{c}} \mathbf{E}^i(Q,\tau)\cdot\bar{\bar{\mathbf{D}}}\left(t-\frac{r}{c}-\tau\right)d\tau,\ \ t-\frac{r}{c}>t_0 \tag{14}$$

where, $t_0 = \frac{r'}{c}$ is the time that takes the wave front to arrive at the diffraction point Q.

$A(r)$ means the spreading factor expressing the power conservation in a tube or strip of rays:

$$A(r) = \begin{cases} \dfrac{1}{\sqrt{r}} & \text{for plane, cylindrical, and conical wave} \\ \sqrt{\dfrac{r'}{r(r'+r)}} & \text{for spherical wave} \end{cases} \tag{15}$$

where, r means the distance between Q and P_r; r' means the curvature radius of incident wave front. For the case of plane wave, cylindrical wave and conical wave, $r' = \infty$; for the case of spherical wave, r' is the distance between Q and source.

$\bar{\bar{\mathbf{D}}}(t)$ denotes the dyadic diffraction coefficient, which is given as

$$\bar{\bar{\mathbf{D}}}(t) = -\hat{\beta}_0'\hat{\beta}_0 D_s(t) - \hat{\phi}'\hat{\phi} D_h(t) \tag{16}$$

where, D_s and D_h is time domain scalar diffraction coefficient deduced in the soft (Dirichlet) and hard (Neumann) boundary condition, respectively; and is given in [14].

Suppose $\hat{s}'$ is a unit vector in the direction of the incident ray path, $\hat{s}$ is that of the diffraction ray path, unit vector $\hat{e}$ is tangent to the edge. Hence, the plane of incidence contains $\hat{s}'$ and $\hat{e}$; and the plane of diffraction contains $\hat{s}$ and $\hat{e}$. These planes are depicted in Figure 2(a). The unit vector $\hat{\phi}'$ and $\hat{\phi}$ is perpendicular to the plane of incidence and the plane of diffraction, respectively, as shown in Figure 2(b); the unit vector $\hat{\beta}_0'$ and $\hat{\beta}_0'$ is parallel to the plane of incidence and the plane of diffraction, respectively. The definitions of these angles are as follows:

$$\begin{cases} \hat{\phi}' = \hat{s}'\times\hat{e} & \hat{\phi}' = \hat{e}\times\hat{s} \\ \hat{\beta}_0' = \hat{s}'\times\hat{\phi}' & \hat{\beta}_0 = \hat{s}\times\hat{\phi} \end{cases} \tag{17}$$

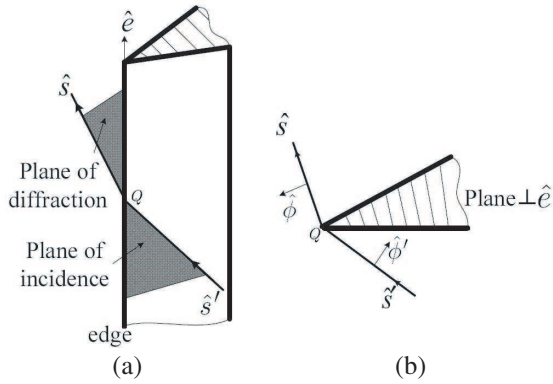

Figure 2. Sketch of the diffraction at a edge.

Adding the wedge diffracted field $\mathbf{E}^d(\mathbf{r},t)$ to the excitation items in (6), we obtain

$$\mathbf{V}_{j,m}^{\mathrm{IE}} = \left\langle \mathbf{f}_m^{\mathrm{IE}}(\mathbf{r}),\, \hat{\mathbf{n}} \times \hat{\mathbf{n}} \times \left(\mathbf{E}^i(\mathbf{r},t) + \mathbf{E}^d(\mathbf{r},t) \right) \right\rangle \big|_{t=t_j} \tag{18}$$

$$\mathbf{V}_{j,m}^{\mathrm{PO}} = \left\langle \mathbf{f}_m^{\mathrm{PO}}(\mathbf{r}),\, \hat{\mathbf{n}} \times \left(\mathbf{H}^i(\mathbf{r},t) + \mathbf{H}^d(\mathbf{r},t) \right) \right\rangle \big|_{t=t_j} \tag{19}$$

where, $\mathbf{H}^d(\mathbf{r},t)$ denotes the diffracted magnetic field. Substituting (18) (19) into (6), we finally obtain the formulation of UTD-PO-TDIE.

$$\begin{bmatrix} \mathbf{Z}_0^{\text{IE-IE}} & \mathbf{Z}_0^{\text{IE-PO}} \\ \mathbf{Z}_0^{\text{PO-IE}} & \mathbf{C}_0^{\text{PO-PO}} \end{bmatrix} \cdot \begin{bmatrix} \mathbf{I}_j^{\mathrm{IE}} \\ \mathbf{I}_j^{\mathrm{PO}} \end{bmatrix} = \begin{bmatrix} \mathbf{V}_j^{\mathrm{IE}} \\ \mathbf{V}_j^{\mathrm{PO}} \end{bmatrix} - \sum_{i=1}^{j} \begin{bmatrix} \mathbf{Z}_i^{\text{IE-IE}} & \mathbf{Z}_i^{\text{IE-PO}} \\ \mathbf{Z}_i^{\text{PO-IE}} & \mathbf{C}_i^{\text{PO-PO}} \end{bmatrix} \cdot \begin{bmatrix} \mathbf{I}_{j-i}^{\mathrm{IE}} \\ \mathbf{I}_{j-i}^{\mathrm{PO}} \end{bmatrix} \tag{20}$$

This is the same, in the form, as the formulation of PO-TDIE.

4. NUMERICAL RESULT

The example is a 10 m × 10 m PEC square plate with a 0.25 m × 0.25 m × 1 m PEC column which lies 1 m away from the plate, shown in Figure 3, as a typical electrically large object with an electrically small thing which has significant features. The incident field is in the waveform of Gaussian pulse with the amplitude of 1 V/m and the bandwidth of 4 lm (light meter) ($f_{\max} = 150$ MHz), the direction of incidence and the polarization is $-z$ and x, respectively. 3920 unknowns are generated, time step is 0.378 lm.

Three cases are considered:

(1) Full TDIE;
(2) PO-TDIE hybrid method, the column is in TDIE region, and the plane is in PO region;
(3) The proposed method, the region division is the same as above.

Figure 4 shows the transient current distribution on the top center of the column. It is evident, from Figure 4, the three curves are nearly the same at the first two large peaks; this is because the early-time response is mainly decided by the incidence and the reflected wave from the plate. The difference appears in the weak oscillatory part. Owing to the contribution of the edge diffracted field, the current distribution of the proposed method is better than that of PO-TDIE.

Adding a load of $50\,\Omega$ on the top center of the column, and the received power as a function of frequency is computed using

$$\tilde{P}(f) = 0.5\left|\tilde{I}(f)\right|^2 R \tag{21}$$

where, $\tilde{I}(f)$ denotes Fourier transformed currents. As shown in Figure 5, in the frequency domain, Compared to PO-TDIE, the agreement between the results of full TDIE and UTD-PO-TDIE is much better.

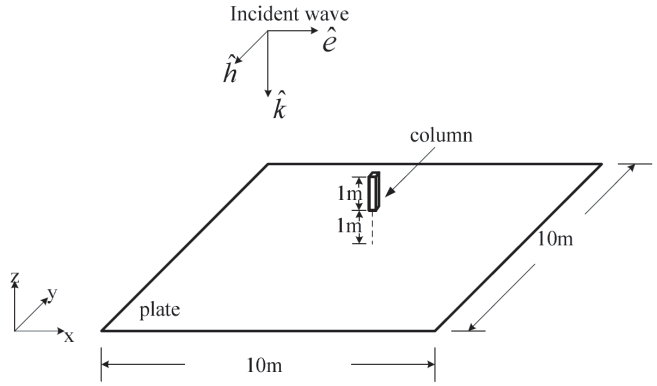

Figure 3. Structure of the PEC column and plate.

Table 1. Contrast of the running times.

	TDIE	PO-TDIE	UTD-PO-TDIE
Unknowns in TDIE region	3920	54	54
Time to fill the impedance matrix (m)	218.2	7.7	7.7
Time to solve the linear equations (m)	178.1	39.1	39.2
Total time (m)	396.4	47.1	47.2

All calculations are accomplished on the Core2 Quad Q9300 CPU, 4 GB Ram PC. Table 1 presents the contrast of the running times (approximate). The cost of UTD-PO-TDIE is nearly the same as PO-TDIE, this illustrate that the accuracy improvement is costless.

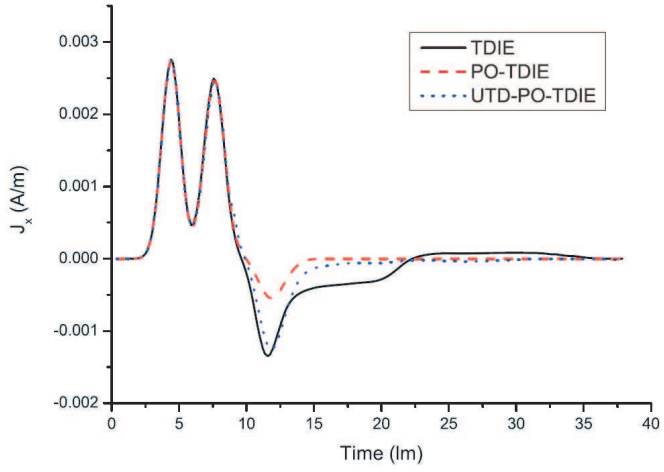

Figure 4. Transient current distribution on the top center of the column.

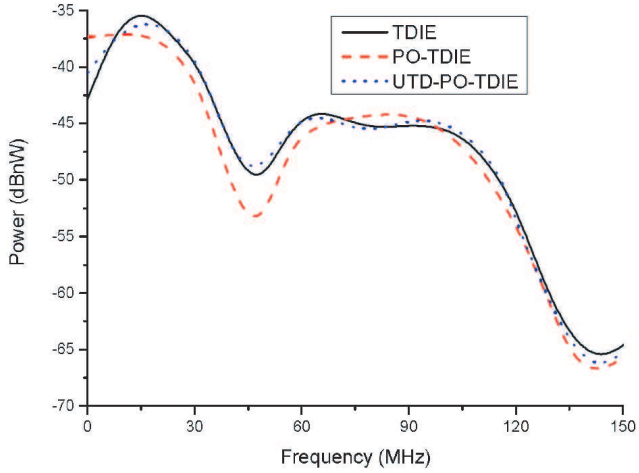

Figure 5. Received power by the top center of the column.

5. DISCUSSION AND CONCLUSION

The impedance matrix of the proposed method is in full agreement with that of PO-TDIE; the enhancement is in the excitation function; therefore, the stability is, theoretically, the same as PO-TDIE.

The computational cost will increase if the geometrical complexity increases, especially considering 2nd order diffraction. However, compared to the cost of solving the impedance matrix, in electrically large applications, it is nearly negligible.

In this paper, we propose a novel UTD-PO-TDIE algorithm, which can enhance the accuracy of PO-TDIE while maintaining the computational complexity. The proposed method is especially suitable for the target with obvious diffraction characters.

While it is clear that this technique works well for simple structure, additional work needs to be undertaken in this area. Interesting issues for further study include:

(1) Extend the diffraction phenomenon to the surface creeping wave,
(2) Enhance the universality of this algorithm.

REFERENCES

1. Bennett, C. L., "A technique for computing approximate impulse response for conducting bodies," Ph.D. thesis, Purdue Univ., Lafayette, Indiana, 1968.
2. Walker, S. P., "Developments in time domain integral equation modeling at imperial college," *IEEE Ant. Prop. Mag.*, Vol. 39, No. 1, 7–19, 1997.
3. Walker, S. P., "Scattering analysis via time domain integral equations: Methods to reduce the scaling of cost with frequency," *IEEE Ant. Prop. Mag.*, Vol. 39, No. 5, 13–20, 1997.
4. Ergin, A., B. Shanker, and E. Michielssen, "The plane-wave time-domain algorithm for the fast analysis of transient wave phenomena," *IEEE Ant. Prop. Mag.*, Vol. 41, No. 4, 39–52, 1999.
5. Shanker, B., A. Ergin, M. Y. Lu, et al., "Fast analysis of transient electromagnetic scattering phenomena using the multilevel plane wave time domain algorithm," *IEEE Trans. Antennas Propagat.*, Vol. 51, No. 3, 628–641, 2003.
6. Yilmaz, A. E., J. M. Jin, and E. Michielssen, "Time domain adaptive integral method for the combined field integral equation," *Proc. IEEE Antennas Propagat S. Int. Symp.*, 543–546, 2003.
7. Yilmaz, A. E., J. M. Jin, and E. Michielssen, "Time domain

adaptive integral method for surface integral equations," *IEEE Trans. Antennas Propagat.*, Vol. 52, No. 10, 2692–2708, 2004.

8. Ren, M., et al., "Coupled TDIE-PO method for transient scattering from electrically large conducting objects," *Electronics Letters*, Vol. 44, No. 4, 258–260, 2008.
9. Walker, S. P. and M. J. Vartiainen, "Hybridization of curvilinear time-domain integral equation and time-domain optical methods for electromagnetic scattering analysis," *IEEE Trans. Antennas Propagat.*, Vol. 46, No. 3, 318–324, 1998.
10. Kouyoumjian, R. G. and P. H. Pathak, "A uniform geometrical theory of diffraction for an edge in a perfectly conducting surface," *Proceedings of the IEEE*, Vol. 62, No. 11, 1448–1461, 1974.
11. Rao, S. M., D. R. Wilton, and A. W. Glisson, "Electromagnetic scattering by surfaces of arbitrary shape," *IEEE Trans. Antennas Propagat.*, Vol. 30, No. 3, 409–418, 1982.
12. Rao, S. M., *Time Domain Electromagnetics*, Academic Press, 1999.
13. Costa, M. F., "Electromagnetic radiation and scattering from a system of conducting bodies interconnected by wires," Ph.D. dissertation, Syracuse University, 1983.
14. Veruttipong, T. W., "Time domain version of the uniform GTD," *IEEE Trans. Antennas Propagat.*, Vol. 38, No. 11, 1757–1764, 1990.
15. Rousseau, P. R. and P. H. Pathak, "Time-domain uniform geometrical theory of diffraction for a curved wedge," *IEEE Trans. Antennas Propagat.*, Vol. 43, No. 12, 1375–1382, 1995.